

Dynamically induced scalar quark confinement

Reinhard Alkofer¹, Christian S. Fischer² and Felipe J. Llanes-Estrada³

¹ Institut für Physik, Karl-Franzens-Universität,
Universitätsplatz 5, A-8010 Graz, Austria

² Institut für Kernphysik, TU Darmstadt,
Schlossgartenstrasse 9, 64289 Darmstadt, Germany

³ Dept. Física Teórica I, Univ. Complutense, Madrid 28040, Spain

Abstract

We employ a functional approach to investigate the confinement problem in quenched Landau gauge QCD. We demonstrate analytically that a linear rising potential between massive quarks is generated by infrared singularities in the dressed quark-gluon vertex. The selfconsistent mechanism that generates these singularities is driven by the scalar Dirac amplitudes of the full vertex and the quark propagator. These can only be present when chiral symmetry is broken. We have thus uncovered a novel mechanism that directly links chiral symmetry breaking with confinement.

More than thirty years after the identification of non-Abelian gauge theory as the appropriate framework to describe the strong interactions we still lack a satisfactory understanding of the confinement phenomenon. Isolated particles with nonvanishing colour charges have not been observed in nature. This fact is supposed to be encoded in the infrared structure of QCD. In the quenched theory a gauge invariant signature of confinement is the area law of the Wilson loop at large distances. This behaviour corresponds to a linear rising potential between static colour charges in the fundamental representation of the gauge group. This signature has been unambiguously verified in lattice gauge QCD, see *e.g.* ref. [1]. However, the dynamical mechanism that generates the Wilson potential is still elusive. Since the underlying long range interaction is provided by gauge dependent objects, this mechanism may have a different appearance in different gauges. In this letter we present such a mechanism for covariant Landau gauge QCD.

The idea of 'infrared slavery', *i.e.* the notion that infrared singularities generate confinement, dates back to the early seventies [2, 3]. Speculations about the infrared behaviour of the running coupling at that time distinguish two cases: (A) the coupling develops an infrared fixed point and (B) the coupling diverges at small or zero momenta. The last possibility has been considered as the driving mechanism for the generation of infrared singularities and quark confinement. Today there is ample evidence from functional approaches that the first possibility is realised in the Yang-Mills sector of Landau gauge QCD: the running coupling freezes out at small momenta [4, 5, 6, 7]. However, this does not imply that the Green's functions of Yang-Mills theory are finite in the infrared: Instead, depending on the number of ghost and gluon legs, many of the one-particle irreducible Green's functions are indeed singular in the limit that all external momenta vanish [7]. In this letter we demonstrate that these singularities also induce a corresponding singularity in the dressed quark-gluon vertex. As a consequence the running coupling defined from this vertex diverges at vanishing renormalization scale, and a linear potential between massive quarks is generated thereby realizing infrared slavery via an infrared singular quark-gluon vertex.

Besides confinement the other fundamental property of infrared QCD is dynamical chiral symmetry breaking, *i.e.* the nonperturbative generation of

quark masses from dynamical interaction with gluons. Lattice QCD tells us that the chiral phase transition and the deconfinement transition take place at a similar temperature [8]. This suggests a relation between confinement and dynamical chiral symmetry breaking, which, however, has not been clarified in detail yet. In this letter we present, based mostly on an analytical calculation, an explicit mechanism that links these two phenomena.

The functional approach we employ for our investigation is given by the tower of Dyson-Schwinger equations for the one-particle irreducible (1PI) Green's functions of QCD [9, 10, 11]. A great advantage of this continuum based formulation as compared to lattice QCD is the analytical access to the infrared behaviour of these functions without finite-volume effects necessarily present in lattice calculations. As has been demonstrated for the propagators of three-dimensional Yang-Mills theory extremely large lattices are mandatory to access the small momentum region where the infrared asymptotic scaling can be identified [12]. The computational costs for a corresponding investigation in four dimensions exceeds current possibilities. This problem is even more severe for higher n -point functions. This underlines the necessity for a continuum based approach to the Green's functions of QCD.

To begin with we shortly summarise previous results for the infrared behaviour of the Green's function in Landau gauge Yang-Mills theory. Gauge fixing in this framework is performed by the standard Faddeev-Popov method supplemented by auxiliary conditions such that the generating functional consists of an integral over gauge field configurations that are contained in the first Gribov region. (The feasibility of this method has been justified in a framework employing stochastic quantisation [13].) The resulting Dyson-Schwinger equations for 1PI-Green's functions have been solved analytically in the infrared to all orders in a skeleton expansion (*i.e.* a loop expansion using full propagators and vertices) [7]. Here we are interested in the case where all external momenta go to zero. Choosing all momenta proportional to each other and requiring for the largest one $p^2 \ll \Lambda_{\text{qcd}}^2$ a self-consistent solution of the whole (untruncated) tower of DSEs is given by [7]

$$\Gamma^{n,m}(p^2) \sim (p^2)^{(n-m)\kappa}, \quad (1)$$

where $\Gamma^{n,m}$ stands for the infrared leading dressing function of a Green's

functions with $2n$ external ghost legs and m external gluon legs. The exponent κ is known to be positive [14]. An important property of the infrared solution (1) is the fact that it is generated by exactly those parts of the DSEs that involve ghost loops [7]. In other words: the Faddeev-Popov determinant dominates the infrared behaviour of non-Abelian Yang-Mills theories. Thus an infrared asymptotic theory can be obtained by ‘quenching’ the Yang-Mills action, *i.e.* setting $\exp(-S_{YM}) \rightarrow 1$ in the generating functional [13]. The solution of this asymptotic theory is given by the power laws (1). Interestingly, this limit is a continuum analogue of the strong coupling limit of lattice gauge theory.

Examples of the general solution (1) are given by the inverse ghost and gluon dressing functions, $\Gamma^{1,0}(p^2) = G^{-1}(p^2)$ and $\Gamma^{0,2}(p^2) = Z^{-1}(p^2)$, respectively. They are related to the ghost and gluon propagators via

$$D^G(p^2) = -\frac{G(p^2)}{p^2}, \quad D_{\mu\nu}(p^2) = \left(\delta_{\mu\nu} - \frac{p_\mu p_\nu}{p^2} \right) \frac{Z(p^2)}{p^2}. \quad (2)$$

The corresponding power laws in the infrared are

$$G(p^2) \sim (p^2)^{-\kappa}, \quad Z(p^2) \sim (p^2)^{2\kappa}. \quad (3)$$

Since κ is positive one obtains an infrared diverging ghost propagator, a behaviour which is necessary to ensure a well defined, *i.e.* unbroken, global colour charge [15]. In Landau gauge an explicit value for κ can be derived from the observation that the dressed ghost-gluon vertex becomes (almost) bare in the infrared [16, 17, 18]. One then obtains $\kappa = (93 - \sqrt{1201})/98 \approx 0.595$ [5, 6, 19], which implies that the gluon propagator vanishes in the infrared. A direct consequence of this behaviour are positivity violations in the gluon propagator and therefore the confinement of transverse gluons [4, 20].

A further important consequence of the solution (1) is the qualitative universality of the running coupling in the infrared. Renormalisation group invariant couplings can be defined from either of the primitively divergent vertices of Yang-Mills-theory, *i.e.* from the ghost-gluon vertex ($gh - gl$), the

three-gluon vertex ($3g$) or the four-gluon vertex ($4g$) via

$$\begin{aligned}
\alpha^{gh-gl}(p^2) &= \frac{g^2}{4\pi} G^2(p^2) Z(p^2) \quad p^2 \xrightarrow{\sim} 0 \quad \mathbf{c}_1/N_c, \\
\alpha^{3g}(p^2) &= \frac{g^2}{4\pi} [\Gamma^{0,3}(p^2)]^2 Z^3(p^2) \quad p^2 \xrightarrow{\sim} 0 \quad \mathbf{c}_2/N_c, \\
\alpha^{4g}(p^2) &= \frac{g^2}{4\pi} [\Gamma^{0,4}(p^2)]^2 Z^4(p^2) \quad p^2 \xrightarrow{\sim} 0 \quad \mathbf{c}_3/N_c.
\end{aligned} \tag{4}$$

Employing the DSE-solution (1) it is easy to see that all three couplings approach a fixed point in the infrared. However, the explicit value of the fixed point, $c_{1,2,3}/N_c$, may be different for each coupling. For a bare ghost-gluon vertex one obtains $\alpha^{gh-gl}(0) \approx 8.92/N_c$ [5]; the other couplings have not been determined yet. Equations (4) underline that indeed the fixed point scenario (A) is realised in the Yang-Mills sector of QCD. In turn this explains the existence of the power law solutions (1): the theory becomes approximately conformal in the far infrared.

We now present a significant extension of this analysis to the quark sector of quenched QCD. To this end we first choose the masses of the valence quarks to be large, *i.e.* $m \geq \Lambda_{\text{QCD}}$. The remaining scales below Λ_{QCD} are those of the external momenta of the Green's functions. Here we are primarily interested in the case where all external momenta go to zero. Then, without loss of generality, one can choose all external momenta to be proportional to one scale p^2 , which is small compared to all other scales in the theory, *i.e.* $p^2 \ll \Lambda_{\text{QCD}}^2$. One can then employ Dyson-Schwinger equations to search for selfconsistent solutions in terms of powers of p^2 .¹

¹Integrals with an infrared power-law enhancement are themselves dominated by infrared integration momenta. We illustrate this with the following simple example, where $\alpha > 1$ is a real number. Consider

$$I(p) = \int_0^\Lambda \frac{dq}{(q+p)^\alpha} = \frac{1}{1-\alpha} ((\Lambda+p)^{1-\alpha} - p^{1-\alpha}) .$$

Then, asymptotically for small p ,

$$I(p) \rightarrow \frac{1}{\alpha-1} \frac{1}{p^{\alpha-1}}$$

and it is the lower integration limit that contributes. Then we just need to subdivide the

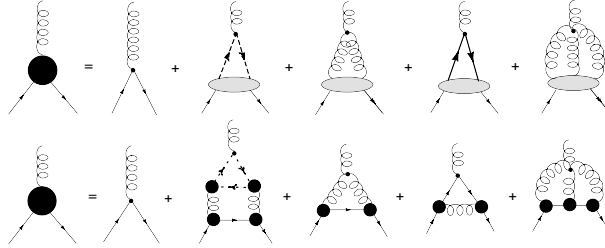


Figure 1: Dyson-Schwinger equation for the quark-gluon vertex. In the first line we show the full equation [21]. The second line shows the lowest order of a skeleton expansion, that already reveals the correct power counting in the infrared. All internal lines in the diagrams represent fully dressed propagators.

We apply this method to the Dyson-Schwinger equation for the full quark-gluon vertex, given diagrammatically in the first line of Fig. 1. In the second line the higher n -point functions of this equation have been expanded to lowest order in a skeleton expansion in terms of full propagators and vertices. The dressed quark-gluon vertex Γ_μ can be decomposed in a basis of twelve tensor structures, which are given explicitly *e.g.* in [22]. Due to momentum conservation the vertex depends only on the two external quark momenta (p_μ, q_μ) or three Lorentz invariants $(p^2, q^2, p \cdot q)$. To analyse the infrared limit of this vertex in the presence of only one external scale $p^2 \ll \Lambda_{\text{QCD}}^2$, we can set $q_\mu = 2p_\mu$ without loss of generality. This leaves us with only four possible tensor structures which can be denoted by

$$\Gamma_\mu(p) = ig \sum_{i=1}^4 \xi_i(p^2) G_\mu^i \quad (5)$$

integration interval

$$\int_0^\Lambda = \int_0^{\lambda_1} + \int_{\lambda_1}^{\lambda_2} + \dots + \int_{\lambda_{n-1}}^{\lambda_n}$$

and it is always the lower (0) limit of the first subinterval that generates the power-law in p . Therefore, for low- p , the q integration is infrared dominated. Another way of putting it is that the integral is divergent with $p = 0$, and keeping finite p regulates it. Then the integral is dominated by momentum scales of order the regulator.

with ξ_i being Lorentz and Dirac scalar functions and

$$G_\mu^1 = \gamma_\mu, \quad G_\mu^2 = \hat{p}_\mu, \quad G_\mu^3 = \hat{\not{p}}\hat{p}_\mu, \quad G_\mu^4 = \hat{\not{p}}\gamma_\mu, \quad (6)$$

where we have normalised the momentum, $\hat{p}_\mu = p_\mu/\sqrt{p^2}$, to ease power counting. Note that G_μ^1 and G_μ^3 have an odd number of γ -matrices, whereas G_μ^2 and G_μ^4 have an even number. Therefore $\xi_{2,4} \neq 0$ only if chiral symmetry is broken.

The internal loops of the skeleton expansion in Fig. 1 are dominated by loop momenta similar to the external scale p^2 due to the denominators of the loop propagators. Thus for $p^2 \ll \Lambda_{\text{QCD}}^2$ the dressing functions of internal propagators and vertices can be approximated by the power laws given in (1). We therefore use (3) for the scaling of the ghost and gluon propagators. The ghost-gluon vertex scales as a constant in the infrared [16, 17, 18]. The internal quark propagator lines can be written as

$$S(p) = \frac{i\not{p} + M(p^2)}{p^2 + M^2(p^2)} Z_f(p^2) \rightarrow \frac{i\not{p} Z_f}{M^2} + \frac{Z_f}{M}. \quad (7)$$

for momenta $p^2 \ll \Lambda_{\text{QCD}}^2$, $M = M(p^2 \rightarrow 0) \gtrsim \Lambda_{\text{QCD}}$ and $Z_f = Z_f(p^2 \rightarrow 0)$. Hereby we assume that neither the quark mass function $M(p^2)$ nor the wave function renormalisation $Z_f(p^2)$ is singular in the infrared [23]. This assumption will be justified below by selfconsistency arguments. From the two tensor structures in (7) the scalar piece turns out to be the leading one in the infrared.

For the internal quark-gluon vertices we can employ the expression (5) with any internal momentum as argument: it contains all possible types of Dirac structures (vector, scalar, and tensor) and any more complicated dependence on external and internal momenta will generate the same powers of external momenta in $\xi_{1..4}$ after integration (for dimensional reasons). To determine the infrared exponents of the quark-gluon vertex we employ the ansatz

$$\xi_1 \sim (p^2)^{\beta_1}, \quad \xi_2 \sim (p^2)^{\beta_2}, \quad \xi_3 \sim (p^2)^{\beta_3}, \quad \xi_4 \sim (p^2)^{\beta_4} \quad (8)$$

for the scaling of the dressing functions of the quark-gluon vertex with momentum. We then substitute this ansatz into the skeleton expansion of the

vertex-DSE and determine the exponents $\beta_{1..4}$ selfconsistently by matching the left and right hand sides. The resulting infrared solution is given by

$$\begin{aligned} \beta_2 &= -1/2 - \kappa, & \beta_1, \beta_3 &\in [(-1/2 - \kappa), (-\kappa)] \\ & & \beta_4 &\in [(-1/2 - \kappa), (1/2 - \kappa)]. \end{aligned} \quad (9)$$

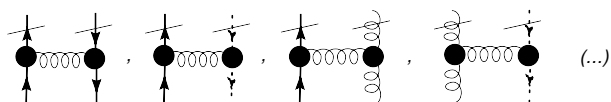
We have checked this analytic solution also in numerical calculations and found that the case

$$\beta_{1..4} = -1/2 - \kappa \quad (10)$$

is realised. The details of this calculation will be presented elsewhere [24].

There are two important remarks here: Firstly, similar to the DSEs in the Yang-Mills sector it is the diagram containing the ghost loop that dominates the right hand side of the equation in Fig. 1. Thus also the infrared behaviour of the quark sector is dominated by effects generated from the Faddeev-Popov determinant. Secondly, the driving tensor structures of the solution (9), (10) are the scalar Dirac amplitude G_μ^2 of the quark-gluon vertex and the scalar (Z_f/M) part of the quark propagator. Both structures are only present when chiral symmetry is broken. If they are absent, as in the case of restored chiral symmetry, one obtains a different solution. We analyse this case below.

Before we discuss the solution (9) further it is important to check that it persists to all orders in the skeleton expansion. Higher order terms in this expansion can be generated by inserting diagrammatical pieces like



into lower order diagrams (all propagators are fully dressed). In ref. [7] we showed that insertions involving pure Yang-Mills propagators and vertices do not change the overall infrared divergence of a given diagram. This is also true for the three pieces involving quark lines: The first one introduces two quark-gluon vertices, two quark propagators and one gluon propagator plus a new integration into a given diagram. This amounts to an additional power of

$$\frac{Z_f^2 (p^2)^{-1-2\kappa+2\kappa-1+2}}{M^2} = \frac{Z_f^2}{M^2} \quad (11)$$

in the external momentum (p^2). A similar result is obtained for the other pieces. Thus diagrammatic insertions of quark lines do not change the infrared behaviour of a given diagram but introduce additional powers of Z_f/M . This implies that the solution (9) is valid to all orders in the skeleton expansion. It is therefore also an infrared solution of the full vertex-DSE.

We wish to add that the infrared divergence presented here has been found under the pretext that all external momenta of the vertex go to zero. However, a more detailed analysis of the vertex-DSE also shows, that the power law must be more general, $(p_3^2)^{-1/2-\kappa}$ in terms of the gluon momentum p_3 . The uniform divergence presented here is therefore a particular case since, once all momenta vanish, also the gluon momentum vanishes. The details of the more general analysis will be presented elsewhere [24].

An important application of our infrared power counting scheme concerns the four-quark 1PI Green's function $H(p)$, which is given in Fig. 2 together with its skeleton expansion. From the terms of the skeleton expansion one obtains $H(p) \sim (p^2)^{-2}$ in the infrared. The well known relation

$$V(\mathbf{r}) = \frac{1}{(2\pi)^3} \int H(p^0 = 0, \mathbf{p}) e^{i\mathbf{p}\mathbf{r}} d^3p \sim |\mathbf{r}| \quad (12)$$

between the static four-quark function $H(p^0 = 0, \mathbf{p})$ and the quark potential $V(\mathbf{r})$ therefore gives a linear rising potential by naive dimensional arguments. A more refined treatment, as described in [25], leads to the same result. Note that already the first term in the skeleton expansion, *i.e.* nonperturbative one-gluon exchange displayed in Fig. 2, generates this result. Since the following terms in the expansion are equally enhanced in the infrared, the string tension will be built up by summing over an infinite number of diagrams. The coefficients of these diagrams will be investigated elsewhere [24].

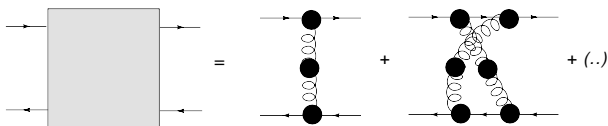


Figure 2: The four-quark 1PI Green's function and the first terms of its skeleton expansion

A further interesting quantity is the running coupling α_{qg} from the quark-gluon vertex. A nonperturbative and renormalisation group invariant definition of this coupling is given by

$$\alpha_{qg}(p^2) = \frac{g^2}{4\pi} \xi_1^2(p^2) Z_f^2(p^2) Z(p^2) \sim \frac{1}{N_c} \frac{1}{p^2}, \quad (13)$$

where ξ_1 dresses the γ_μ -part of the vertex, see Eq. (5). With the exponents $\beta_2 = \beta_1 = -1/2 - \kappa$, as obtained in our numerical solutions, we find by power counting that the coupling is proportional to $1/p^2$. Thus, contrary to the couplings (4) from the Yang-Mills vertices, we find this coupling to be singular in the infrared, i.e. 'infrared slavery' is realised.

So far we found quark confinement in the chirally broken phase of quenched QCD. Our power counting scheme worked in this case, because only one external momentum and no other small scales were present. This is also true in the chirally symmetric phase of (quenched) QCD with massless valence quarks. The solution (1) for the pure Yang-Mills sector is still valid in this case. In the quark sector all tensor structures in the quark propagator and the quark-gluon vertex that violate chiral symmetry have to disappear, in particular ξ_2 and ξ_4 have to vanish identically. We are thus left with

$$S(p) = \frac{i\not{p}}{p^2} Z_f(p^2), \quad \Gamma_\mu(p) = ig \sum_{i=1,3} \xi_i(p^2) G_\mu^i \quad (14)$$

for the quark propagator and for the quark-gluon vertex. On general grounds $Z_f(p^2)$ cannot be infrared singular and can be treated as a constant. We then obtain

$$\beta_1 = \beta_3 = -\kappa \quad (15)$$

for the exponents in (8). This solution no longer leads to a confining potential. One obtains $H(p) \sim (p^2)^{-1}$ for the infrared behaviour of the four-quark function. This leads to a potential of Coulomb type

$$V(\mathbf{r}) = \frac{1}{(2\pi)^3} \int H(p^0 = 0, \mathbf{p}) e^{i\mathbf{p}\mathbf{r}} d^3p \sim \frac{1}{|\mathbf{r}|}. \quad (16)$$

Also the resulting running coupling from the quark-gluon vertex is no longer diverging but goes to a fixed point in the infrared

$$\alpha_{qg}(p^2) = \frac{g^2}{4\pi} \xi_1^2(p^2) Z_f^2(p^2) Z(p^2) \sim \frac{1}{N_c}, \quad (17)$$

similar to the couplings from the Yang-Mills vertices. The restoration of chiral symmetry is therefore directly linked with the disappearance of infrared slavery and confinement.

To summarise: We presented an analysis of quenched QCD in the covariant Landau gauge. Our results show that infrared slavery is at work, though in a different fashion than has been assumed in many previous investigations. It is not a gluon propagator with a $1/p^4$ -behaviour in the infrared that confines quarks. Instead the gluon propagator is even vanishing at zero momentum. However, there is enough infrared strength in the quark-gluon vertex to compensate for this: We found a linear rising potential from the four-quark Green's function. This potential is triggered by scalar Dirac amplitudes in the quark propagator and quark-gluon vertex. However, since $\beta_1 = \beta_2$, the potential also contains vector contributions. An answer to the old question of scalar vs. vector confinement is therefore a nontrivial dynamical issue. Corresponding numerical results will be published elsewhere [24]. Finally, we wish to emphasise again that if chiral symmetry is restored the confining solution disappears. As a result we have uncovered a novel link between dynamical chiral symmetry breaking and confinement.

Acknowledgements

This work has been supported by the Deutsche Forschungsgemeinschaft (DFG) under contracts Al 279/5-1 and Fi 970/7-1 and the Spanish grant FPA 2004-02602.

References

- [1] G. S. Bali and K. Schilling *Phys. Rev.* **D46** (1992) 2636.
- [2] S. Weinberg *Phys. Rev. Lett.* **31** (1973) 494.
- [3] D. J. Gross and F. Wilczek *Phys. Rev.* **D8** (1973) 3633.
- [4] L. von Smekal, R. Alkofer, and A. Hauck *Phys. Rev. Lett.* **79** (1997) 3591.
- [5] C. Lerche and L. von Smekal *Phys. Rev.* **D65** (2002) 125006.

- [6] J. M. Pawłowski, D. F. Litim, S. Nedelko, and L. von Smekal *Phys. Rev. Lett.* **93** (2004) 152002.
- [7] R. Alkofer, C. S. Fischer, and F. J. Llanes-Estrada *Phys. Lett.* **B611** (2005) 279.
- [8] F. Karsch and E. Laermann, arXiv:hep-lat/0305025.
- [9] C. D. Roberts and A. G. Williams *Prog. Part. Nucl. Phys.* **33** (1994) 477.
- [10] R. Alkofer and L. von Smekal *Phys. Rept.* **353** (2001) 281.
- [11] C. S. Fischer *J. Phys. G: Nucl. Part. Phys.* **32** (2006) R253.
- [12] A. Cucchieri, T. Mendes, and A. R. Taurines *Phys. Rev.* **D67** (2003) 091502.
- [13] D. Zwanziger *Phys. Rev.* **D69** (2004) 016002.
- [14] P. Watson and R. Alkofer *Phys. Rev. Lett.* **86** (2001) 5239.
- [15] T. Kugo, arXiv:hep-th/9511033.
- [16] J. C. Taylor *Nucl. Phys.* **B33** (1971) 436.
- [17] A. Cucchieri, T. Mendes, and A. Mihara *JHEP* **12** (2004) 012.
- [18] W. Schleifenbaum, A. Maas, J. Wambach, and R. Alkofer *Phys. Rev.* **D72** (2005) 014017.
- [19] D. Zwanziger *Phys. Rev.* **D65** (2002) 094039.
- [20] R. Alkofer, W. Detmold, C. S. Fischer, and P. Maris *Phys. Rev.* **D70** (2004) 014014.
- [21] W. J. Marciano and H. Pagels *Phys. Rept.* **36** (1978) 137.
- [22] J. S. Ball and T.-W. Chiu *Phys. Rev.* **D22** (1980) 2542.
- [23] C. S. Fischer and R. Alkofer *Phys. Rev.* **67** (2003) 094020.
- [24] R. Alkofer, C. S. Fischer, F. J. Llanes-Estrada and K. Schwenzer, arXiv:0804.3042 [hep-ph].
- [25] D. Gromes *Zeit. Phys.* **C11** (1981) 147.